Fluorescence Based Measurement of Temperature Profiles During Polymer Processing

KALMAN B. MIGLER *and* ANTHONY J. BUR

National Institute of Standards and Technology
Polymers Division
Gaithersburg, Maryland 20899

We describe a novel noninvasive method to measure temperature profiles during processing. A key feature is the use of a temperature-sensitive fluorescent dye that is incorporated into the polymer resin at dopant levels. By monitoring spectral features of this dye, we can effectively measure its temperature. A focusing technique that we call "confocal fluorescent optics" then allows us to measure the temperature as a function of position into the resin. We present results of critical tests of the device. Namely we test the spatial resolution and its ability to measure a linear temperature profile in a quiescent polymer. Finally, we present the first on-line temperature profile measurements, carried out in a circular die at the exit of a twin screw extruder. Temperature gradients on the order of 5°C/mm in a polyethylene resin are observed between the outer wall and the center of the die.

INTRODUCTION

The temperature of a polymer resin is a critically important parameter during all stages of processing. In the case of thermoplastics, if the temperature is too high, thermal degradation of the polymer occurs; whereas if it is too low, the increased viscosity may lead to excessive energy consumption and reduced product quality. In the case of thermoset materials, chemical reaction can occur prematurely when the temperature is too high. Yet despite its importance, it is extremely difficult to obtain an accurate temperature measurement.

The difficulty lies primarily in the high viscosities and the low thermal conductivities of polymer melts. The high viscosities give rise to significant shear-heating effects during processing. The low thermal conductivity prevents this shear-induced heating from fully dissipating during time scales relevant to processing. Consequently, spatial nonuniformities in temperature are easily generated. As the resin temperature near the wall of an extruder barrel may be quite different from that in the bulk of the sample, single point measurement techniques are problematic. Even in the case of a simple geometry such as flow through a slit, the situation is complex because the velocity field is coupled with the temperature distribution. In addition to the usual plug type flow that is created in this geometry because of shear thinning, one must consider that regions of higher shear are at elevated temperature because of shear induced heating, thus further reducing the viscosity in these high shear regions.

There have been numerous studies devoted to the prediction and measurement of radial temperature profiles in flowing polymer melts (1–11). Experimentally, most of the work has involved the measurement in a circular die shortly past the screw of an extruder (1–5, 7–9). In some cases a retractable probe is used in which a thermocouple is progressively inserted into the flow channel (1–6). Such a device is commercially available. In other cases, a bridge is built into a channel onto which a multi-probe assembly is placed (7–9). These studies have uncovered spatial temperature variations on the order of 10°C to 30°C in several different materials such as PVC (1, 2, 8), polyethylene (2–4, 9), polypropylene (5), and polycarbonate (7). While the above studies are unsuitable for temperature measurement in a screw channel, Esseghir and Sernas have manufactured a cam-driven probe that is synchronized to move in and out of a screw channel (6).

These invasive measurement techniques have several inherent problems. In order to withstand the forces generated during flow, the thermocouples must be mounted on a strong structural support. These supports alter the flow of the polymer both up and downstream. Upstream alteration of the flow is particularly serious because it alters the point of origination of the polymer at the thermocouple. Additionally, the supports create local shear heating and suffer from thermal conduction effects between the barrel and the probe.

An infrared pyrometer is an example of a noninvasive temperature measurement. However, since the infrared radiation is generated by all objects, includ-

ing the probe, the barrel and the far wall, it is difficult to carry out a temperature profile measurement (5, 12, 13). Additionally, mapping out a temperature profile from IR data is a mathematically ill-posed problem (13).

There is a clear need for a noninvasive technique that only measures the temperature of the resin and can carry out temperature profile measurements. In this work, we describe a novel noninvasive method to measure temperature profiles during processing. A key feature of this method is the use of a temperature-sensitive fluorescent dye that is incorporated into the polymer resin at dopant levels. By monitoring relevant spectral features of this dye, we can measure its temperature. A focusing technique that we call "confocal fluorescent optics" then allows us to measure the temperature as a function of distance into the resin. We test the spatial resolution of the device and test its ability to measure a linear temperature profile in a quiescent polymer. Finally, we present the first on-line temperature profile measurements, carried out in a circular die at the exit of a twin screw extruder.

FLUORESCENT BASED TEMPERATURE MEASUREMENTS

Fluorescent dyes have been used to monitor the state of the polymer in numerous applications such as mixing (14), injection molding (15), and flow slippage (16). In order to measure temperature, we utilize the fact that there exist several classes of molecules whose emission spectrum is strongly temperature-dependent. Examples of these dyes are excimer formers (17–23), molecular rotors (24), rare-earth compounds (25–28) and others (29). The fluorescent dyes can be doped into the polymer resin at low mass fraction $c < 1 \times 10^{-5}$ (mass fraction) so as not to disturb other properties of the medium. We use the excimer forming dye bis(-pyrene) propane (BPP) whose structure is shown in *Fig. 1*. In the excimer-forming molecules, there are two fluorescent monomers (pyrene) attached by a flexible spacer (14, 15). When one monomer is excited by ultraviolet radiation, it can decay by several paths: it can fluoresce with rate constant k_f; it can decay nonradiatively; or it can associate with the other monomer to form an excimer state at rate constant k_a. An excimer state is an excited electronic state caused when an excited monomer rotates about the flexible bond and overlaps with the other one. In analogy to the case of a monomer, an excimer can fluoresce with rate constant k_f', it can decay nonradiatively, or it can dissociate back to an excited monomer and a ground state monomer with rate constant k_d. The excimer fluorescence occurs at longer wavelengths than the monomer and is broad and featureless. The ratio of the excimer to monomer fluorescence is given by (18):

$$\frac{I_e}{I_m} = \frac{k_f' k_a}{k_f (k_d + 1/\tau_o')} \tag{1}$$

where τ_o' is lifetime of the excimer. The temperature dependence of this ratio is dominated by k_d and k_a. In order to form an excimer state once a given monomer becomes excited, the two fluorescent monomers must reorient and overlap before the monomer decays by fluorescence or nonradiative decay. The rate at which the monomers can overlap, k_a, is governed by the "microviscosity" of the medium. In polymeric materials, k_a is governed by the WLF equation above T_g (19–23), indicating the importance of segmental mobility and free volume. An increase in temperature would cause an increase in k_a, and in the case when the dissociation is negligible, $k_d \ll (\tau_o')^{-1}$, then I_e/I_m is an increasing function of temperature. Once an excimer state is formed, dissociation is governed by an activation energy required to break the intramolecular bond. At higher temperatures, the dissociation rate k_d becomes greater. When k_d becomes large enough, *Eq. 1* shows that I_e/I_m becomes a *decreasing* function of temperature (15).

Our on-line temperature measurements are based on the dependence of I_e/I_m with temperature for the dye BPP in polyethylene. We first calibrate the samples in the quiescent state. Samples for calibration purposes are prepared by first dissolving the dye BPP into toluene. Next the toluene solution is poured into a shallow evaporation disk containing polyethylene pellets. As the solvent evaporates, the dye coats the surface of the pellets. These coated pellets are then dry mixed with untreated ones to reach a final typical BPP mass fraction of 2×10^{-6}. Final blending of the dye into the resin is accomplished during the actual extrusion. The spectra of BPP in polyethylene are shown in *Fig. 2* at two temperatures. The peak that occurs at 480 nm is due to the excimer fluorescence, whereas the peak at 400 nm is due to the monomer

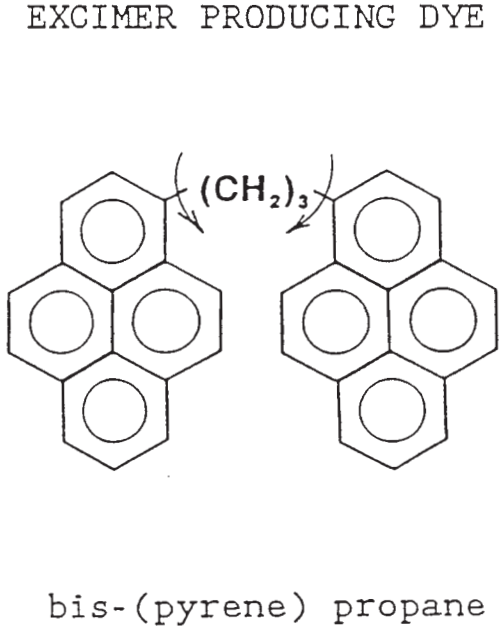

Fig. 1. Chemical structure of the excimer producing dye bis-pyrene propane.

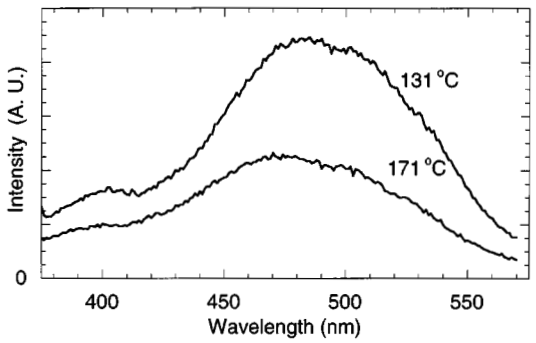

Fig. 2. Spectral intensity of fluorescence emission in arbitrary units (A.U.) of the dye molecule BPP in polyethylene at two temperatures (linear scale).

fluoresence. For purposes of calibration and temperature measurement, the key feature of these curves is the difference in the ratio of excimer to monomer fluorescence. (At room temperature, the intensity of the monomer fluorescence is much greater than that of the excimer fluorescence.)

The calibration of the dye-resin system is carried out with the same optics and instrumentation as the on-line measurements. In order to produce fast measurements, we measure light intensity at only the two wavelength bands corresponding to the excimer and monomer fluorescence as shown in *Fig. 3*. Light from a commercial arc lamp is collimated by condenser lens (A) and is filtered by a bandpass filter (B), which only transmits in a band of wavelengths that correspond to the absorption wavelength of the dye molecule. This filtered light (excitation light) is focused by lens (C) onto one end of a bifurcated fiber optic bundle (D). The excitation light diverges from the fiber bundle at the common end and is focused onto the sample. A fraction of the resulting fluorescent light travels into the other arm of the bifurcated fiber optic bundle (E). Upon exiting the fiber-optic bundle, the light is resolved into the monomer and excimer components through the dichroic beam splitter (F) and the band-pass filters and cut-on filters (G). The intensity of the light at these two spectral components is measured by the photomultiplier tubes whose outputs go to a dual channel photon counter. The photon counter sends the computer the intensity of light at each wavelength band. It is important to note that the ratios obtained by this technique do not correspond to absolute spectral ratios, but rather they are a function of the bandpass filters and other optical elements used in these measurements. The details of the focusing optics will be described later.

Once the material is blended (see next section), it is put into a temperature controlled chamber with an optical access. *Figure 4* shows a plot of I_e/I_m as a function of temperature for the probe BPP in polyethylene. The estimated standard uncertainty in temperature is 0.5°C and in I_e/I_m ratio is 0.5%. As discussed above, there is a peak in I_e/I_m as a function of temperature due to the relative importance of k_a compared to k_d. As the polyethylene processing occurs at temperatures above 140°C, we are interested in the region of the curve where I_e/I_m is a decreasing function of temperature. The absolute intensities of I_e and I_m show discontinuities at T_m, ~110°C because of the strong optical scattering associated with the crystallization. However, the trends in the ratio measurements below T_m are still correct. The semi-crystalline nature of polyethylene below T_m complicates the discussion of the rate constants given above, and we will not discuss this region of the curve any further. The data is reproducible upon heating and subsequent cooling, indicating that no thermal degradation effects are occurring on the time scale of several hours at temperatures up to about 220°C. Owing to photo-bleaching effects, it is important to limit the total exposure time when using a quiescent sample. (This is not a concern in flowing materials.) In an extruder, one must consider the effect of pressure on the calibration curve. In the current experiments, the pressure is low enough that these effects are small (~2°C).

In practice, the on-line determination of temperature via the fluorescent technique is to first calibrate the specific polymer-dye system as a function of tem-

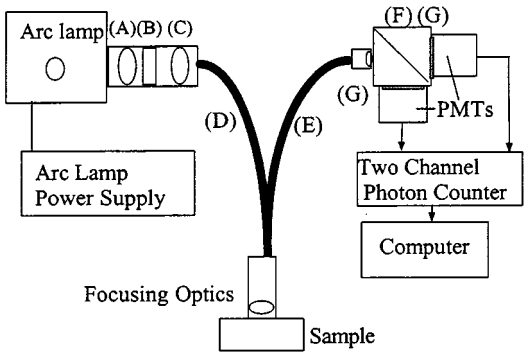

Fig. 3. Diagram of the optics used for the measurement of the ratio of excimer to monomer production. The details of the mechanics and the optics inside the bolt are shown in Figs. 5 and 6.

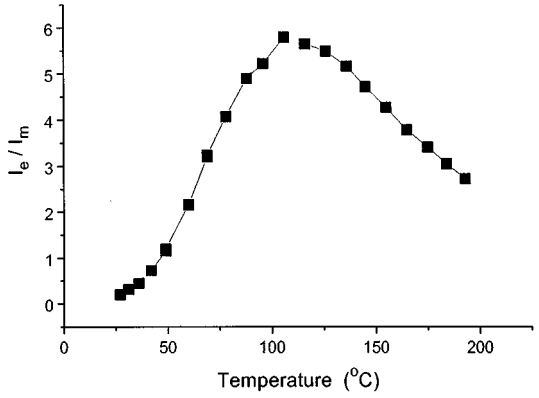

Fig. 4. Calibration curve showing the ratio of excimer to monomer fluorescence as a function of temperature for the dye BPP in polyethylene.

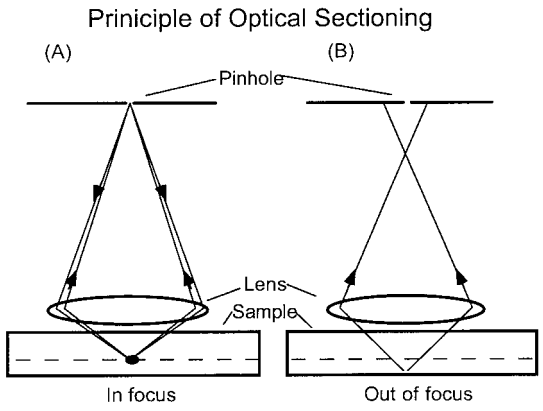

Fig. 5. Principle of fluorescent confocal optics. The focal plane is represented by the dashed line: (A) Excitation light from a pinhole is imaged by the lens onto the sample. The resulting fluorescent light is then focused by the same lens back onto the pinhole. (B) Fluorescent light from an out-of-focus region is mostly rejected by the pinhole.

perature. From this calibration curve, one generates a simple functional form to describe the temperature dependence. During on-line temperature measurements, one uses this functional form to back out the temperature. Prior work indicates that small fluorescent probe molecules are not aligned by shear flow (30).

FLUORESCENT CONFOCAL OPTICS

In order to measure a temperature profile, we must use optics that detect fluorescence from only a small portion of the sample. Also, we must be able to scan this point of measurement in the radial direction. These two requirements can be met through the use of fluorescent confocal optics (31) as illustrated in *Fig. 5*. The basic principle is that excitation light is incident from the pinhole onto the lens and then focused onto the sample. A fraction of the resulting fluorescent light then follows the reverse path back into the pinhole. The power of this simple optical arrangement is that most of the fluorescent light that comes back into the pinhole was generated at the focal point in the sample. Light from out-of-focus regions is efficiently rejected by the pinhole. *Figure 5B* shows that most of the fluorescent light generated from a point beyond the focal plane does not reach the pinhole. By translating the lens and pinhole up and down, the focal point moves, and different regions of the sample are probed. In order to minimize the depth of field, a large numerical aperture lens is used; Snell's law then fixes the distance between the lens and sample to be much less than that between the fiber and lens.

A challenge in the implementation of a temperature profiling device into an extruder port hole is the small working space available, as well as the high temperatures and pressures that are routinely used. Therefore we need an optical design that is as simple as possible. We use the optical layout shown in *Fig. 6*. This device employs a bifurcated fiber optic cable as shown in *Fig. 2*. The functionality of the pinhole (as seen in *Fig. 5A*) is realized simply by the end of the optical fiber bundle, which is 1 mm in diameter. The distance between the lens and the fiber optic bundle is about 22 mm, which is far greater than the focal length of the lens. Since the light emerging from the fiber optic bundle diverges to a diameter greater than the lens diameter, an iris is used to block stray excitation light.

The iris and lens assembly are shown in *Fig. 7A* where the steel piece is darkened to further absorb stray light. The iris is made by machining a rib into the steel piece. The iris and lens assembly can screw onto the fiber optic end-piece (*Fig. 7B*). The fiber optic lens assembly fits into the drilled out hole in the bolt (*Fig. 7C*). An important feature of the bolt is the 2-mm-thick sapphire window, which allows optical access into the polymer. This bolt was custom made by Dynisco. The bolt was pressure and temperature tested separately at 420°C and 34.5 MPa (5000 psi) and simultaneously at 250°C and 34.5 MPa (5000 psi).

In order to carry out the profiling, the entire optical assembly (i.e., the fiber optic end-piece, iris and sapphire lens) must be able to translate back and forth. The mechanical translation of the optics is carried out by a micrometer, which is attached through a pair of yokes to the fiber optic end-piece (*Fig. 7C*). Then by using the micrometer to scan the sliding bolt insert back and forth, the temperature at different points in the sample can be measured. A future version of this device will include a motorized micrometer.

Before using this apparatus in a polymer extruder, we must first carry out optical tests to ascertain that it is performing properly. There are two tests that we need to perform. The first is a test of the optical resolution, and the second is of the ability of the appa-

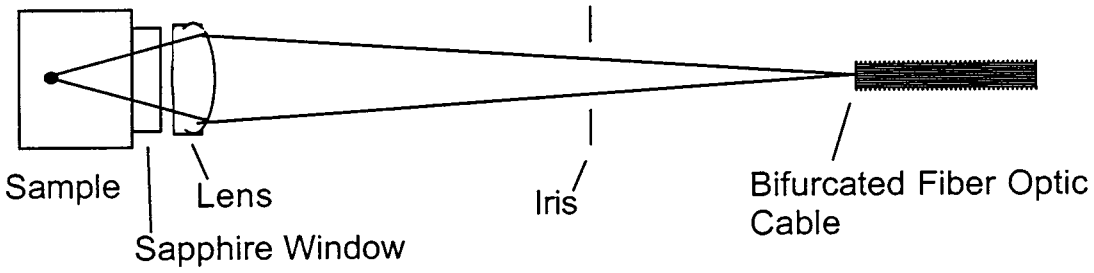

Fig. 6. Optical layout: The lens, iris and the end-piece of the fiber optic cable are one rigid unit that can translate back and forth relative to the sample and sapphire window.

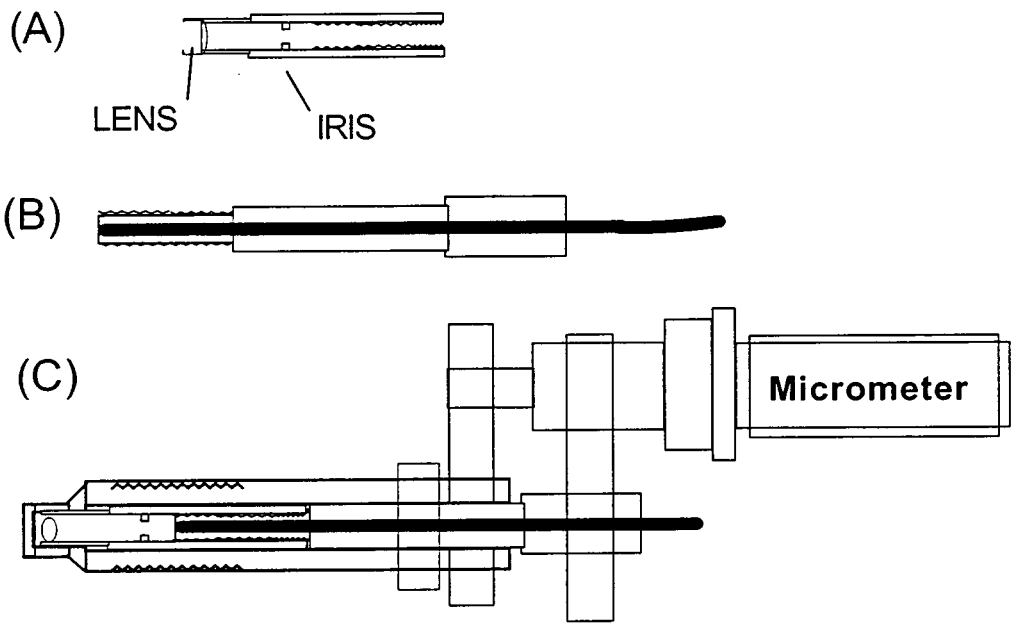

Fig. 7. Mechanical design of the bolt-sized optics.

ratus to measure a temperature profile. We fabricated a test chamber as shown in *Fig. 8*. To measure the spatial resolution, we dope the fluorescent molecule BPP into polydimethyl siloxane (PDMS), chosen in this case because it is an optically transparent room temperature melt. We carry out these measurements at room temperature. We place a piece of anodized (blackened) aluminum into the polymer that absorbs the excitation beam. We can then translate this piece of aluminum closer (or further) away from the bolt. When the anodized aluminum is moved from a distance x to a distance $x+dx$ away from the bolt, there will be an increase in the fluorescent signal due to the doped polymer that occupies the volume between x and $x+dx$. Thus the change in signal between x and $x+dx$ is a measure of the fluorescence that emanates from this slab of space. In *Fig. 9A*, we show the fluorescent intensity as a function of the position of the anodized aluminum. The estimated uncertainty is 0.3% I_m. As described above, the derivative of this curve gives the fluorescent intensity emanating from a given point, as shown in *Fig. 9B*. The estimated standard uncertainty in *Fig. 9B* is 6×10^3 (s mm)$^{-1}$. The width of the peak is about 1 mm, which sets the optical resolution of the device. The maximum range we can achieve when the lens is pressed against the sapphire window is 4 mm. Using the bolt micrometer, we can pull the lens away from the sapphire window and carry out the same scans. By measuring the resulting position of the

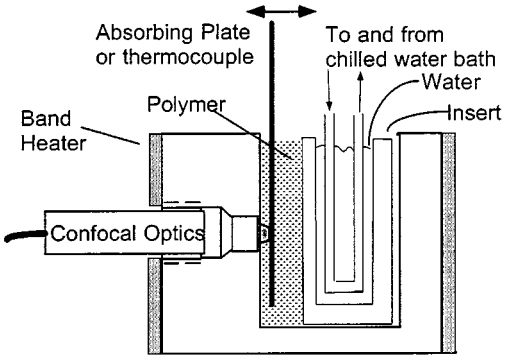

Fig. 8. Side view of the temperature profile test cell. To measure the optical resolution, the absorbing plate translates back and forth.

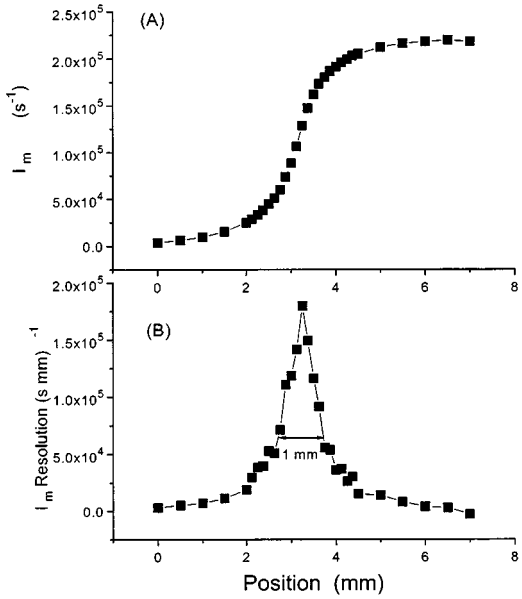

Fig. 9. (A) Fluorescent intensity as a function of position of the absorbing aluminum plate. (B) The spatial resolution of the above optics, as measured by the derivative of the above plot.

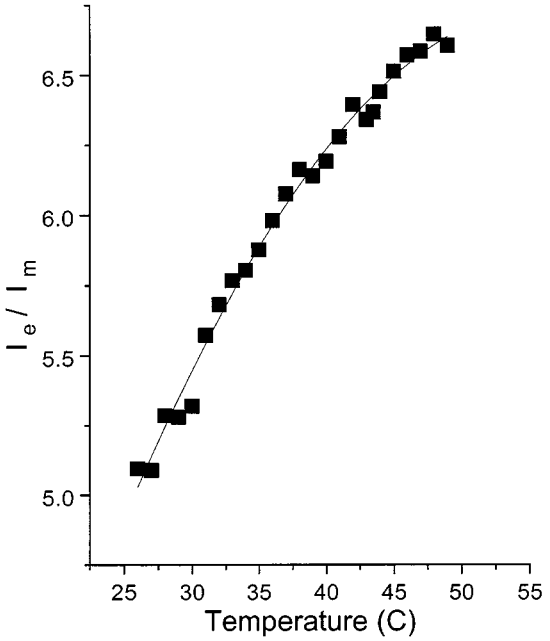

Fig. 10. Calibration curve for the ratio of excimer to monomer fluorescence of BPP in PDMS as a function of temperature.

peak, we can determine the relationship between the measurement position and the distance between the window and lens. Owing to index of refraction effects, the distance between the lens and the window does not have a one-to-one correspondence with the measurement position. This effect is accounted for in all subsequent sections.

The next optical test is to measure a temperature profile near room-temperature conditions. In the absence of a temperature gradient, the optically measured temperature must also be constant. First, we calibrate the dye BPP in PDMS. For a series of temperatures, as measured by a thermocouple inserted into the polymer, we measured the ratio of excimer to monomer fluorescence, as shown in *Fig. 10*. The estimated standard uncertainty in temperature is 0.1°C and that in the ratio is 0.5. The scanning procedure is then to position the micrometer to a given point and simultaneously measure the excimer and monomer fluorescence. From the calibration curve, one determines the temperature at that point. The micrometer is moved to the next position and the procedure is repeated. If optical absorption of excitation light is not significant over the range of measurement, we anticipate that the excimer and monomer signals will not change appreciably in response to the change in focal position (as long as the focal position is within the sample). In *Fig. 11*, the optically measured temperature deviates by less than 0.2°C (which sets the expanded uncertainty for this measurement). I_e and I_m do not show significant variation either.

Next, we need to test the ability of the device to measure a temperature profile. We can create a temperature gradient in the test cell by heating one end of the sample and cooling the other. *Figure 8* shows that a

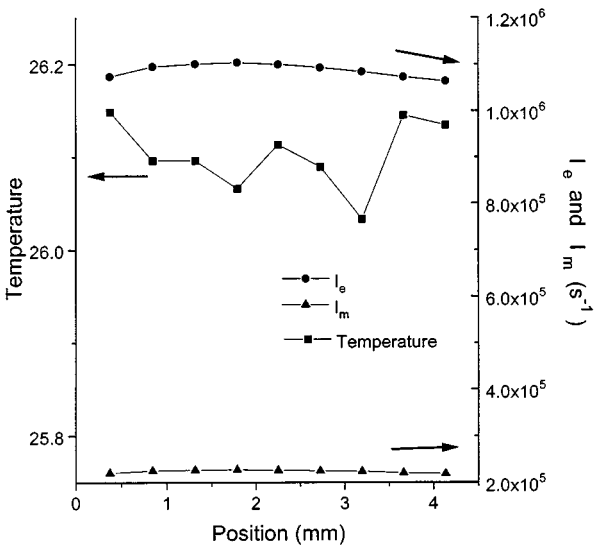

Fig. 11. Temperature measurement in the absence of a temperature gradient.

band heater is used to heat the aluminum test cell, thus warming the polymer in the area adjacent to the bolt. A temperature controller and thermocouple placed in the aluminum block are used in conjunction with the band heater to provide a stable temperature. In order to cool the opposite side, we utilize chilled water circulating through copper tubing. The tubing is placed in the drilled out area of an aluminum insert. Free standing water, which acts as the thermal conductor between the copper tubing and the aluminum insert, is also placed in the drilled out area. We can translate a thin wire thermocouple back and forth and easily measure the temperature profile within the sample. In *Fig. 12*, we compare two curves—one generated by translating the thermocouple, and the other obtained by the fluorescent confocal optics technique. The estimated standard uncertainty in temperature is 0.2°C. There is a close overlap between the two measured curves, which gives us confidence in the capabilities

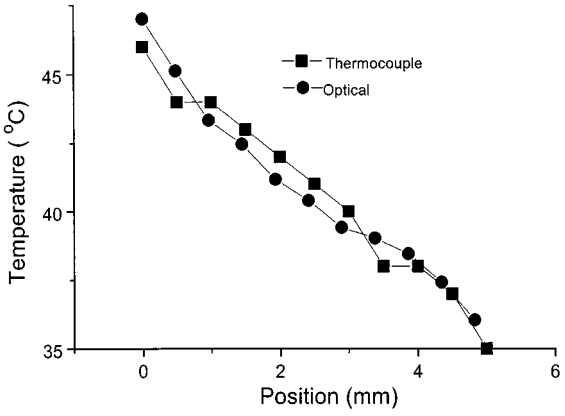

Fig. 12. Measurement of temperature profile of quiescent PDMS, comparing the optical technique with a thermocouple.

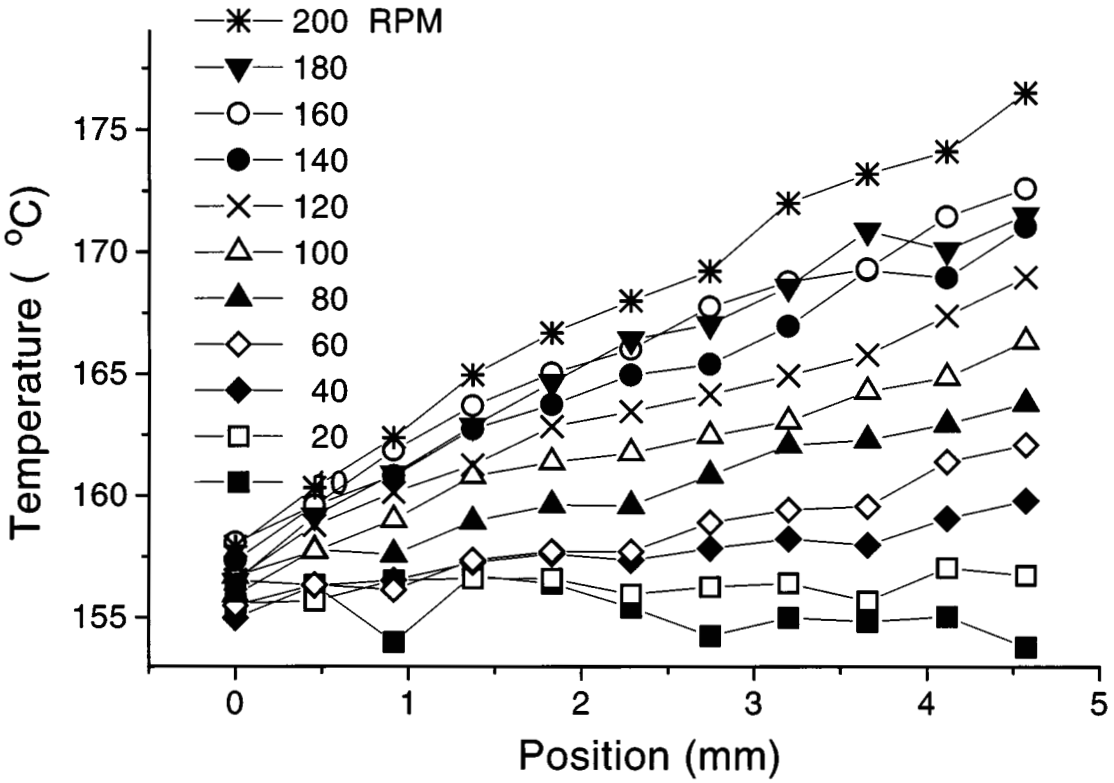

Fig. 13. Measurement of temperature profiles in the exit rod-die of a twin screw extruder.

of the device. This demonstrates that the device can measure a linear temperature profile. Additional numerical work confirms that it can also measure more complex profiles.

IN-LINE TEMPERATURE MEASUREMENTS

The in-line testing was carried out using the BPP dye doped into a Dow polyethylene 640-I (32). The BPP dye was dissolved in toluene and then poured into a 200 gram batch of the PE. The toluene was allowed to evaporate, leaving a coating of the dye on the pellets. These pellets were then dry mixed with undoped pellets so that a molar concentration of 5×10^{-7} was achieved.

The extrusion was carried out in a Haake torque rheometer with a conical co-rotating twin screw attachment. The optical temperature measurements were performed in a rod die situated at the exit of the extruder. The point of measurement is situated upstream of the 2 mm nozzle. The diameter of the tube at the point of measurement is 8 mm, which is roughly twice as large as the range of the optical probe. Since there is roughly a circular symmetry, one only needs to be able to measure over half the diameter. At 90 degrees to the port used for the optical temperature probe, we placed a standard temperature/pressure probe.

In the first series of in-line runs, both the barrel and die set-point temperatures were 160°C. We varied the screw rotation speed, waited several minutes, and carried out temperature profile measurements. The feed rate is set by a metering feeder. For the runs at 10 and 20 rotations per minute (rpm), the feed rate was 32 g/min. For the runs at 40 through 200 rpm, the feed rate was 65 g/min. By keeping the feed rate constant (for the later 9 runs) and varying the screw speed, we were able to isolate the effects of shear heating from those of polymer throughput. *Figure 13* shows the results of these measurements. In this graph, position 0 corresponds to a measurement at the bolt, while that at 4 mm corresponds to a measurement at the center of the die. The estimated random error in the data 0.2°C. The run-to-run repeatability is ±1°C. The effects of shear heating are clearly visible in this series of runs. At the lowest rpm, the temperature profile is quite small, possibly within the noise of the method. However, as the rpm is increased, the difference in temperature between the wall and the center of the die becomes much larger. At 200 rpm, the temperature difference is about 18° between the wall and the center. This indicates clearly that a melt thermocouple or IR thermometry gives an incomplete picture of the temperature of the polymer resin. The lesson from this set of runs is that the polymer temperature at the center of the die is dominated by the fast flow from the extruder, which is at an elevated temperature because of shear heating. The temperature nearer the wall is composed of a slower moving polymer, which has time to be cooled by the wall. These measurements indicate that shear heating in this 8 mm

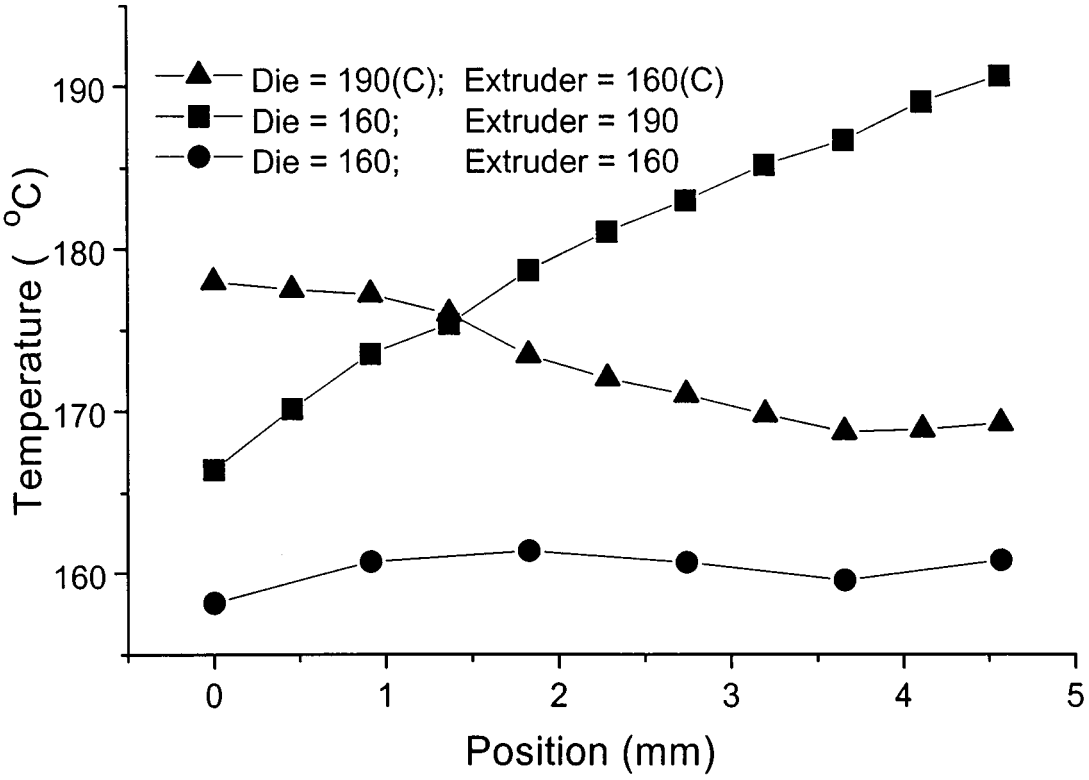

Fig. 14. Measurement of temperature profile when the die and barrel are at different temperatures.

diameter section of the die is weak relative to the shear heating in the barrel; otherwise we would expect to see a stronger temperature rise at the boundary of the die.

In a second test, we were interested to see the effects of changing the temperature of the die relative to that of the twin screw. Frequently in polymer processing, different zones of an extruder or die are maintained at different temperatures. The question is, how does the temperature of an upstream zone affect the temperature of a downstream one. *Figure 14* shows that this effect can be quite large. In the first run (circle data points) the screw rotation is turned off and the temperature profile of the die is measured at a set point of 160°C. In the second and third runs, the screw speed is set to 60 rpm, and the metering feeder is set to a feed rate of 80 g/min. The solid square data points correspond to a run in which we keep the barrel at 190°C while the die is maintained at only 160°C. As expected, the temperature at the center of the die corresponds to that of the fast moving melt emerging from the die, while the temperature at the edge corresponds to the slower-moving polymer near the edge, which has had enough time to cool down. The triangles correspond to the opposite case of setting the barrel temperature to 160°C and increasing the die temperature to 190°C. Again we measure a temperature profile, this time with the temperature near the wall higher than that near the center. Note that the overall temperature difference in this case is about 11°, compared to the gradient of 24° that was observed in the previous case. This is what we expect by considering that the shear heating in the barrel can raise the temperature at the center of the flow. Additionally, the effect of shear heating is smaller in the case where the barrel temperature is higher (decreased viscosity at elevated temperatures leads to decreased shear heating).

CONCLUSION

In summary, we have demonstrated that the optical sensor is capable of measuring temperature profiles. Furthermore, the ease with which we can generate temperature profiles indicates that temperature gradients are ubiquitous in polymer processing, and that the ability to measure them is key to the understanding of polymer behavior in extrusion.

There are several avenues for further research. One area is to improve the optics in order to enhance the resolution and increase the range of measurement. We will also apply this technology in various applications, such as temperature profiles in the barrel of an extruder, where we will look directly over the screw. We also believe that this device may be quite useful in injection molding, where very large temperature gradients are known to exist.

ACKNOWLEDGMENTS

We gratefully acknowledge the assistance we received from Leo Barren of Dynisco in the fabrication of the bolt.

REFERENCES

1. H. T. Kim and E. A. Collins, *Polym. Eng. Sci.*, 11, 83 (1971).
2. E. A. Collins and F. E. Filisko, *AiChe J.*, 16, 339 (1970).
3. T. W. McCullough and B. T. Hilton, *SPE ANTEC*, 927 (1992).
4. T. W. McCullough and M. A. Spalding, *SPE ANTEC*, 412 (1996).
5. X. Shen and R. Malloy, *SPE ANTEC*, 918 (1992).
6. M. Esseghir and V. Sernas, *SPE ANTEC*, 54 (1991).
7. I. Bruker, C. Miaw, A. Hasson, and G. Balch, *Polym. Eng. Sci.*, 27, 504 (1987).
8. H. T. Kim and J. P. Darby, *SPE J.*, 26, 31 (1970).
9. W. Schlaffer, J. Schijf, and H. Janeschitz-Kriegl, *Plastics and Polymers*, 193 (1971).
10. S. M. Dinh and R. C. Armstrong, *AiChe J.*, 28, 295 (1982).
11. T. J. Lindt, *Polym. Eng. Sci.*, 29, 471 (1989).
12. C. C. Chen, *SPE ANTEC*, 931 (1992).
13. J. X. Rietveld and G.Y. Lai, *SPE ANTEC*, 834 (1994).
14. A. J. Bur, F. W. Wang, C. L. Thomas, and J. L. Rose, *SPE ANTEC*, 135 (1993).
15. A. J. Bur and F. M. Gallant, *Polym. Eng. Sci.*, 31, 1365 (1991).
16. K. B. Migler, H. Hervet, and L. Leger, *Phys. Rev. Lett.*, 70, 287 (1993).
17. J. B. Birks, *Photophysics of Aromatic Molecules*, Wiley, New York (1970).
18. Z. A. Zachariasse, G. Duveneck, and R. Busse, *J. Am. Chem. Soc.*, 106, 1045 (1984).
19. L. Bokobza, C. Pham-Van-Cang, L. Monnerie, J. Vandendriessche, and F. C. De Schryver, *Polymer*, 30, 45 (1989).
20. D. P. Jing, L. Bokobza, L. Monnerie, P. Collart, and F. C. De Schryver, *Polymer*, 30, 443 (1989).
21. D. P. Jing, L. Bokobza, P. Sergot, L. Monnerie, P. Collart, and F. C. De Schryver, *Polymer*, 31, 110 (1990)
22. Freeman, L. Bokobza, P. Sergot, L. Monnerie, and F. C. De Schryver, *J. Lum.*, 49, 259 (1991).
23. F. Laupretre, L. Bokobza, and L. Monnerie, *Polymer*, 34, 468, (1993).
24. R. O. Luotfy and B. A. Arnold, *J. Phys. Chem.*, 86, 4205 (1982).
25. M. L. Bhaumik, *J. Chem. Phys.*, 40, 3711 (1964).
26. P. Kolodner, A. Katzir, and N. Hartsough, *Appl. Phys. Lett.*, 42, 749 (1983).
27. E. J. Edgerton, A. Nef, W. Millikin, W. Cook, and D. Baril, *Sol. St. Tech.*, 84 (1982).
28. Luxtron Thermometer, Luxtron, Inc.
29. B. T. Campbell, T. Liu, and J. P. Sullivan, AIAA 94-2483.
30. A. J. Bur *et al.*, *Macromolecules*, 25, 3503 (1992).
31. *Confocal Microscopy*, T. Wilson, ed., Academic Press (1990).
32. Certain equipment and instruments or materials are identified in this paper in order to adequately specify the experimental conditions. Such identification does not imply recommendation by the National Institute of Standards and Technology, nor does it imply that the materials are necessarily the best available for the purpose.

Received Feb. 21, 1997
Revised April 1997

NOTES